European Journal of Chemistry

View Journal Online
View Article Online

Crystal structure of *bis*(1,8-dibenzoyl-7-methoxynaphthalen-2-yl) terephthalate: Terephthalate phenylene moiety acts as bidentate hydrogen acceptor of bidirectional C-H···π non-classical hydrogen bonds

Kikuko Iida, Rei Sakamoto, Kun Li, Miyuki Kobayashi, Hiroaki Iitsuka, Noriyuki Yonezawa and Akiko Okamoto *

Department of Organic and Polymer Materials Chemistry, Tokyo University of Agriculture and Technology, 2-24-16 Nakamachi, Koganei, Tokyo, 184-8588, Japan
kikumail@galaxy.dti.ne.jp (K.I.), aokamoto.apr9@gmail.com (R.S.), s212813v@st.go.tuat.ac.jp (K.L.), miyuki.kobayashi184638@gmail.com (M.K.), hiroaki.iitsuka185268@gmail.com (H.I.), yonezawa@cc.tuat.ac.jp (N.Y.), aokamoto@cc.tuat.ac.jp (A.O.)

** Corresponding author at: Department of Organic and Polymer Materials Chemistry, Tokyo University of Agriculture and Technology, 2-24-16 Nakamachi, Koganei, Tokyo, 184-8588, Japan.*
e-mail: aokamoto@cc.tuat.ac.jp (A. Okamoto).

RESEARCH ARTICLE

10.5155/eurjchem.12.2.147-153.2114

Received: 01 March 2021
Received in revised form: 16 April 2021
Accepted: 17 April 2021
Published online: 30 June 2021
Printed: 30 June 2021

KEYWORDS

Aggregation
Weak interactions
Conformation analysis
Aromatic ring structure
Bidentate hydrogen acceptor
Bidirectional C-H···π interactions

ABSTRACT

The title compound lies about a crystallographic inversion centre located at the terephthalate moiety. The two *peri*-benzoylnaphthalene units having atrope chirality are also situated centrosymmetrically. In the two *peri*-benzoylnaphthalene moieties, two benzoyl groups are substituted at 1 and 8 carbons of the naphthalene ring in *anti*-orientation. Then two absolute configurations of *peri*-benzoylnaphthalene moieties are consequently assigned as complementary to each other, *i.e.*, one unit has *R,R*-configuration and the other *S,S*-one, respectively. The two benzoyl groups in *peri*-benzoylnaphthalene moiety and the terephthalate phenylene ring are non-coplanarly located against the naphthalene ring. The dihedral angles of each benzene ring of two benzoyl groups and terephthalate unit with the naphthalene ring are 73.73 and 75.96, and 71.79°. In molecular packing, several kinds of weak interactions are responsible to induce three-dimensional molecular network. Especially, the synergetic effect realized through the bidentate hydrogen acceptor function in bidirectional C-H···π non-classical hydrogen bonds by the terephthalate phenylene ring moiety plausibly plays the determining role.

Cite this: *Eur. J. Chem.* **2021**, *12(2)*, 147-153 **Journal website**: www.eurjchem.com

1. Introduction

Weak interactions in the solid of organic molecular substances have acquired interests and the revaluation in the scientific area over the last two decades [1-3]. Indeed, weak interactions have been established as essential features in influencing the chemical, physical, and biological activity properties of materials [4-21], by determining their three-dimensional single molecular structure and spatial organization of molecular assembly. A number of papers and reviews have been dedicated to the crystallographic and theoretical study and consequently the analysis of halogen interactions and nonclassical hydrogen bonds such as C-H···X (X = Polar atom) and C-H···π hydrogen bonds have drastically increased over recent years, emphasizing the applicability and usefulness of weak interactions to scientific disciplines [22-30].

Congested molecules of accumulated aromatic rings have unique spatial structural restriction that the aromatic rings are compellingly arranged in non-coplanar manners. This structural constraint suggests that the contribution of parallel overlap of aromatic rings, *i.e.*, π···π stacking, is extremely small. In this consequence, other weak interactions play relatively leading roles in the stabilization of the molecular packing. From this point of view, crystals of compounds of non-coplanarly accumulated aromatic rings can be expected to emphasize the contributions of rather weak non-covalent bonding interactions other than π···π stacking interactions or classical hydrogen bonds as structure determining factors. Based on the observation results of crystal structural analysis, the method for evaluating the actual stabilizing interactions of aromatic-ring-bearing molecules in solid states should be developed. The authors have investigated synthesis, reaction behavior, and analysis of spatial organization of single molecular and accumulation states of *peri*-aroylnaphthalene homologous compounds in which two aroyl groups are substituted at the adjacent inner carbons of the naphthalene ring [31-34], accompanying with various related compounds [35,36].

ISSN 2153-2249 (Print) / ISSN 2153-2257 (Online)
https://dx.doi.org/10.5155/eurjchem.12.2.147-153.2114

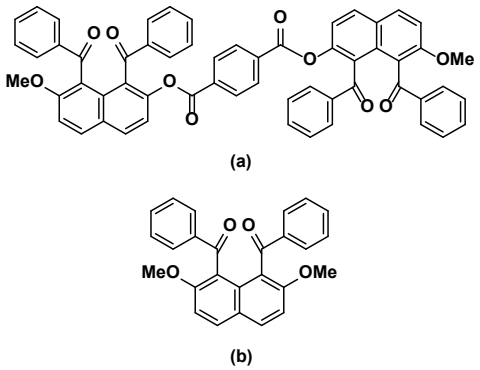

Figure 1. (**a**) Title compound and (**b**) the homologous compound.

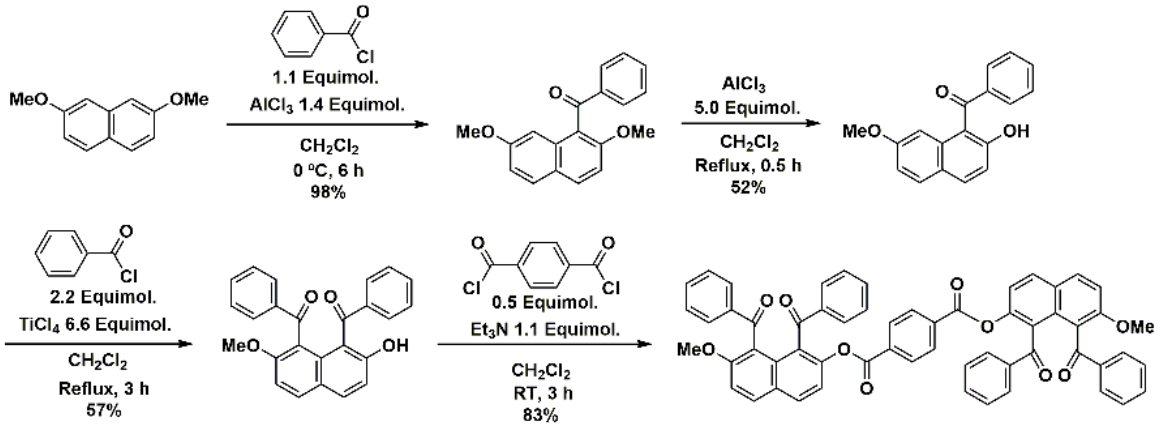

Scheme 1. Synthesis of title compound.

In particular, the authors have reported the crystal structures of these compounds as nearly a hundred articles. *peri*-Aroylnaphthalene compounds have non-coplanarly accumulated structure of aromatic rings and the dihedral angles between aromatic rings are influenced by substituents on the aromatic rings [31]. As a part of the authors' ongoing studies, herein, the X-ray crystal structure of the title compound, an aromatic-ring-accumulated organic substance composed of two 1,8-dibenzoylnaphthalene units and a terephthalate moiety, is reported and consequently the correlation among spatial organization of single molecule, molecular aggregation structure, and non-covalent bonding interactions *via* comparison with 1,8-dibenzoyl-2,7-dimethoxynaphthalene [37] is discussed (Figure 1).

2. Experimental

2.1. Instrumentation and materials

^{1}H NMR spectra were recorded on a JEOL JNM-AL300 spectrometer (300 MHz) and a JEOL JNM-ECA500 spectrometer (500 MHz). ^{13}C NMR spectra were recorded on a JEOL JNM-AL300 spectrometer (75 MHz) and a JEOL JNM-ECA500 spectrometer (125 MHz). Chemical shifts were reported as the delta scale in ppm relative to $CHCl_3$ (δ = 7.29 ppm) for ^{1}H NMR and $CDCl_3$ (δ = 77.7 ppm) for ^{13}C NMR. Chemical shifts were reported as the delta scale in ppm relative to DMSO (δ = 2.50 ppm) for ^{1}H NMR and DMSO-d_6 (δ = 39.7 ppm) for ^{13}C NMR. Elemental analyses were carried out by using a SUMIGRAPH NCH-22 elemental analyzer. IR spectra were recorded on a JASCO FT/IR-4100 spectrometer. High-resolution FAB mass spectra were recorded on a JEOL MStation (MS700) ion trap mass spectrometer in positive ion mode. All reagents were of commercial quality and were used as received. Solvents were dried and purified using standard techniques [38].

2.2. Synthesis

The title compound was prepared the following synthetic procedures presented in Scheme 1. Synthetic procedures of 2,7-dimethoxynaphthalene [39], 1-benzoyl-2,7-dimethoxynaphthalene [40] and 1-benzoyl-2-hydroxy-7-methoxynaphthalene [41] have been reported in the literatures.

2.2.1. Synthesis of 1,8-dibenzoyl-2-hydroxy-7-methoxy naphthalene

Benzoyl chloride (0.44 mmol, 0.05 mL), $TiCl_4$ (1.32 mmol, 0.14 mL) and dichloromethane (0.5 mL) were placed into a 10 mL flask, followed by stirring at room temperature. To the reaction mixture thus obtained, 1-benzoyl-2-hydroxy-7-met hoxynaphthalene (0.2 mmol, 56 mg) was added. After the reaction mixture was stirred under reflux conditions for 3 h, it was poured into iced water (30 mL) and the mixture was extracted with chloroform (10 mL × 3). The combined extracts were washed with brine. The organic layers thus obtained were dried over anhydrous $MgSO_4$. The solvent was removed under reduced pressure to give a cake (yield 57%). The crude product was purified by column chromatography (ethyl acetate:hexane, *v*:*v*, 1:2, isolated yield 36%).

1, 8-dibenzoyl-2-hydroxy-7-methoxynaphthalene: Color: Colorless. Yield: 57%. M.p.: 225.0-226.0 °C. FT-IR (KBr, ν, cm^{-1}): 3246 (OH) (phenol), 2940 (CH_3) (sp^{3}C-H), 1669 (C=O) (ketone), 1641 (C=O) (ketone), 1620 (Ar) (naphthalene), 1596 (Ar) (phenyl), 1577 (Ar) (phenyl), 1513 (Ar) (phenyl), 1451 (OCH_3)

Table 1. Crystal data and details of the structure refinement for title compound.

Parameters	Title compound
Empirical formula	$C_{58}H_{38}O_{10}$
Formula weight	894.88
Temperature (K)	173
Crystal system	Monoclinic
Space group	$P2_1/c$
a, (Å)	7.798(4)
b, (Å)	14.957(7)
c, (Å)	19.498(9)
b, (°)	96.058(6)
Volume (Å^3)	2261.5(18)
Z	2
ρ_{calc} (g/cm^3)	1.314
μ (mm^{-1})	0.09
F(000)	932
Crystal size (mm^3)	0.20 × 0.20 × 0.20
Radiation	MoKα (λ = 0.71070)
2Θ range for data collection (°)	2.503 to 25.998
Index ranges	$-9 \le h \le 9$, $-17 \le k \le 17$, $-23 \le l \le 24$
Reflections collected	15616
Independent reflections	4320 [R_{int} = 0.061, R_{sigma} = 0.617]
Data/restraints/parameters	4320/0/307
Goodness-of-fit on F^2	1.094
Final R indexes [I≥2σ (I)]	R_1 = 0.1673, wR_2 = 0.4454
Final R indexes [all data]	R_1 = 0.1798, wR_2 = 0.4394
Largest diff. peak/hole (e Å^{-3})	0.83/-0.61
Flack parameter	-0.6(10)

Table 2. Hydrogen bond geometry (Å, °) *.

D-H···A	D-H	H···A	D···A	∠D-H···A
C14-H14···O1 ^{i}	0.95	2.36	3.3052	175
C15-H15···O5 ^{ii}	0.95	2.59	3.4513	151
C22-H22···Cg ^{iii}	0.95	2.78	3.6247	149

* Symmetry code: (i) -1+*x*, *y*, *z*; (ii) 1-*x*, -1/2+*y*, 1/2-*z*; (iii) -*x*, 1/2+*y*, 1/2-*z*; Cg is C27-C28-C29-C27-C28-C29 ring.

(ether), 1362 (OCH_3) (ether), 1269 (Ar-O) (ether), 1175 (CH_3-O) (ether), 1011 (CH_3-O) (ether). ^{1}H NMR (300 MHz, DMSO-d_6, δ, ppm): 3.62 (s, 3H, CH_3-O), 7.13 (d, J = 9.0 Hz, 1H, Ar-H), 7.37 (m, 5H, Ar-H), 7.49-7.58 (m, 6H, Ar-H), 7.99 (d, J = 9.0 Hz, 1H, Ar-H), 8.08 (d, J = 9.3 Hz, 1H, Ar-H), 10.15 (s, 1H, O-H). ^{13}C NMR (75 MHz, DMSO-d_6, δ, ppm): 56.8 (1C, CH_3-O), 111.1 (1C, Ar-C), 116.5 (1C, Ar-C), 118.2 (1C, Ar-C), 124.7 (1C, Ar-C), 128.6 (2C, Ar-C), 129.1 (2C, Ar-C), 129.3 (2C, Ar-C), 130.3 (1C, Ar-C), 132.5 (1C, Ar-C), 132.8 (1C, Ar-C), 133.0 (1C, Ar-C), 133.1 (1C, Ar-C), 138.9 (1C, Ar-C), 155.0 [1C, Ar-C(OH)], 156.4 [1C, Ar-C(OCH_3)], 196.9 (1C, C=O), 197.2 (1C, C=O). HRMS (FAB, *m/z*): calcd. for $C_{25}H_{19}O_4$, 383.1284; found, 383.1283.

2.2.2. Synthesis of bis(1,8-dibenzoyl-7-methoxynaphthalen-2-yl)terephthalate

The title compound was prepared by treatment of a mixture of 1,8-dibenzoyl-2-hydroxy-7-methoxynaphthalene (0.2 mmol, 76 mg), terephthaloyl dichloride (0.11 mmol, 22 mg), and triethylamine (0.22 mmol, 0.03 mL) in dichloromethane (0.5 mL). After the reaction mixture was stirred at rt for 3 h, it was poured into water (30 mL) and the mixture was extracted with chloroform (10 mL×3). The combined extracts were washed with brine. The organic layers thus obtained were dried over anhydrous $MgSO_4$. The solvent was removed under reduced pressure to give cake (yield 83%). The crude product was purified by recrystallization from acetonitrile and colorless platelet crystals suitable for X-ray diffraction were obtained (isolated yield 30%).

Bis(1,8-dibenzoyl-7-methoxynaphthalen-2-yl) terephthalate: Color: Colorless. Yield: 83%. M.p.: 316.0-316.5 °C. FT-IR (KBr, ν, cm^{-1}): 1739 (C=O) (ester), 1658 (C=O, Ar) (ketone, naphthalene), 1612 (Ar) (phenyl), 1598 (Ar) (phenyl), 1582 (Ar) (phenyl), 1510 (Ar), 1452 (CH_3-O) (ether), 1260 (Ar-O) (ether), 1175 (CH_3-O) (ether), 1015 (CH_3-O) (ether). ^{1}H NMR (300 MHz, $CDCl_3$, δ, ppm): 3.73 (s, 6H, CH_3-O), 7.21 (t, J = 7.5 Hz, 4H, Ar-H), 7.33-7.40 (m, 14H, Ar-H), 7.49 (t, J = 7.2 Hz, 2H, Ar-H), 7.65 (d, J = 7.2 Hz, 4H, Ar-H), 7.71 (d, J = 7.2 Hz, 4H, Ar-H), 8.02 (d, J = 9.0 Hz, 2H, Ar-H), 8.07 (d, J = 9.3 Hz, 2H, Ar-H). ^{13}C NMR (125 MHz, $CDCl_3$, δ, ppm): 56.6 (1C, OCH_3), 113.5 (1C, Ar-C), 119.5 (1C, Ar-C), 122.9 (1C, Ar-C), 126.6 (1C, Ar-C), 128.2 (1C, Ar-C), 128.3 (1C, Ar-C), 129.3 (2C, Ar-C), 129.5 (2C, Ar-C), 130.0 (1C, Ar-C), 131.7 (1C, Ar-C), 132.4 (1C, Ar-C), 132.5 (1C, Ar-C), 133.0 (1C, Ar-C), 133.3 (1C, Ar-C), 138.1 (1C, Ar-C), 138.6 (1C, Ar-C), 147.5 (1C, Ar-C), 156.5 [1C, Ar-C(OCH_3)], 163.0 [1C, Ar-C(O-C=O)], 195.1 (1C, O=C-O), 197.0 (1C, O=C). Anal. calcd. for $C_{58}H_{38}O_{10}$: C, 77.84; H, 4.28. Found: C, 77.82; H, 4.36%.

2.3. X-ray diffraction analysis

For the crystal structure determination, the single crystal of the title compound was used for data collection on a four circle Rigaku RAXIS RAPID diffractometer (equipped with a two-dimensional area IP detector). The graphite-monochromated MoKα radiation (λ = 0.71070 Å) was used for data collection. The lattice parameters were determined by the least-squares method on the basis of all reflections with $F^2 > 2\sigma(F^2)$. Crystal data, data collection and structure refinement details are summarized in Table 1. The data collection and cell refinement were performed using *PROCESS-AUTO* software [42]. The data reduction was performed using *CrystalStructure* [43]. The structures were solved by direct methods using *SIR2004* [44] and refined by a full-matrix least-squares procedure using the program *SHELXL97* [45]. All H atoms were found in a difference map and were subsequently refined as riding atoms, with the aromatic C-H = 0.95 Å and methyl C-H = 0.98 Å, and with U_{iso}(H) = 1.2U_{eq} (C). The hydrogen bond geometries of the title compound are listed in Table 2. Crystallographic data of title compound has been deposited with the Cambridge Crystallographic Data Centre as Supplementary publication no. CCDC-2063371.

3. Results and discussion

Single molecular structure of the title compound is exhibited in Figure 2.

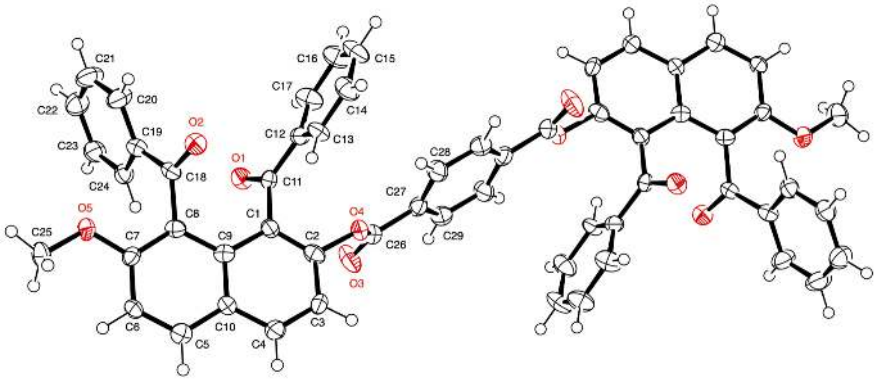

Figure 2. Molecular structure of title compound, showing the atom-numbering scheme. The displacement ellipsoids are drawn at the 50% probability level.

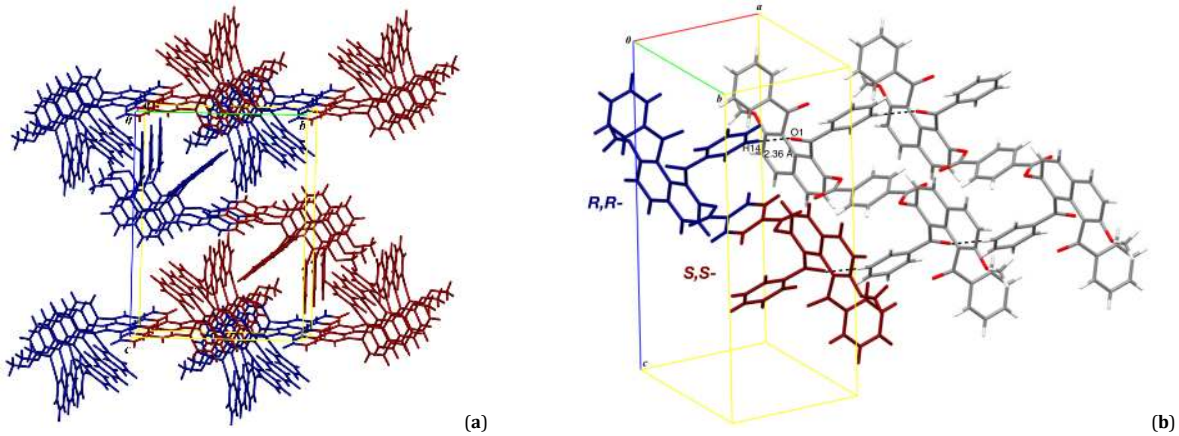

Figure 3. Aggregation structure of *-R,R-R,R-R,R-* and *-S,S-S,S-S,S-*configurated columns (a) and C-H(sp²)...O(=C) non-classical hydrogen bonds between identically configurated dibenzoylnaphthalene units along *a*-axis. (b) *R,R-* and *S,S-*isomers are expressed as blue and red molecules, respectively.

The dinaphthyl terephthalate molecule lies about a crystallographic inversion centre located at the terephthalate phenylene ring so that the asymmetric unit contains one-half of the molecules. Thus, the two *peri*-benzoylnaphthalene units are situated centrosymmetrically with respect to the centre of terephthalate phenylene ring. The spatial configurations of the two *peri*-benzoylnaphthalene moieties are assigned to *R,R*-form and *S,S*-form, respectively. The two benzoyl groups in *peri*-benzoylnaphthalene moiety and the terephthalate phenylene ring are non-coplanarly located to the naphthalene ring. The dihedral angles of each benzene ring with the naphthalene ring are 73.73° for the outer benzoyl group, 75.96° for the inner benzoyl group, and 71.79° for the central terephthalate phenylene moiety. The five benzene rings in the molecule align in stacking manner toward alternative sides against naphthalene planes.

In the molecular packing, *peri*-benzoylnaphthalene units are stacked forming *-R,R-R,R-R,R-* and *-S,S-S,S-S,S-*configurated columns (blue and red molecules) along the *a*-axis direction (Figure 3a). The naphthalene ring interdigitates with the oppositely configurated one in the adjacently aligned column, and *vice versa*, to make both configurated naphthalene moieties overlap alternatively. In addition, each column has been found to possess C-H(sp²)···O(=C) non-classical hydrogen bonds between identically configurated neighbouring dibenzoylnaphthalene isomeric units. These C-H(sp²)···O(=C) non-classical hydrogen bonds are formed between benzoyl groups nearer to the terephthalate phenylene ring (C14-H14···O1; 2.36 Å) (Figure 3b). Besides, C-H(sp²)···O(-Me) non-classical hydrogen bonds are displayed to connect identically configurated isomeric dibenzoylnaphthalene units situated in adjacent columns to the bundle pillars. These C-H(sp²)···O(-Me) non-classical hydrogen bonds are formed between aromatic hydrogen atoms of the inner benzoyl group and the oxygen atom of the methoxy group (C15-H15···O5; 2.59 Å). On the other hand, C-H(sp²)···π (terephthalate) non-classical hydrogen bonds link the oppositely configurated isomeric diaroyl naphthalene units between columns (Figure 4). Moreover, the C-H(sp²)···π (terephthalate) nonclassical hydrogen bonds are found between aromatic hydrogen atoms of outside benzoyl groups on the dibenzoylnaphthalene moiety and the terephthalate phenylene ring (C22-H22···C_g; 2.78 Å).

The authors' group has already reported the crystal structure of a homologous compound, *i.e.*, 1,8-dibenzoyl-2,7-dimethoxynaphthalene, one of the simplest homologues in the authors' series of *peri*-aroylnaphthalene compounds (Figure 5) [37]. In the crystal of the homologous compound, the molecules show chirality caused by atrope isomerization as well as the title compound. Furthermore, molecules are located on a twofold rotation axis. Therefore, the two benzoyl groups are situated in an *anti*-orientation and the dihedral angle between the mean planes of the benzene ring and the naphthalene ring system is 80.25(6)°. The phenyl and carbonyl groups are arranged almost coplanarly. Figure 6a shows the molecular packing structure in which *R,R-* and *S,S-*isomeric molecules are expressed as blue and red molecules, respectively. The crystal packing is stabilized by (methoxy)C-H···O(=C) and C-H(sp²)···O(=C) non-classical hydrogen bonds (C14-H14B···O1 = 2.39 Å; C12-H12···O1 = 2.60 Å) and π···π stacking interaction between benzoyl benzene rings [centroid-centroid and interplanar distances are 3.6383 (10) and 3.294 Å, respectively].

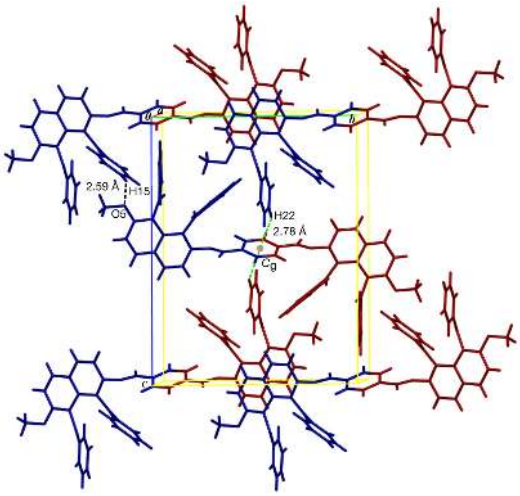

Figure 4. C-H(sp²)···O(-Me) and C-H(sp²)···π(terephthalate) non-classical hydrogen bonds between the columns along *c*-axis. *R,R*- and *S,S*-isomers are expressed as blue and red molecules, respectively.

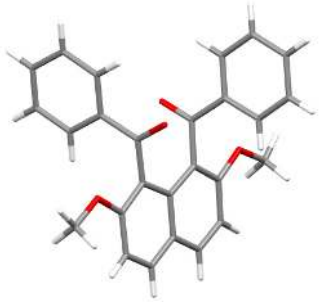

Figure 5. Single molecular structure of 1,8-dibenzoyl-2,7-dimethoxynaphthalene.

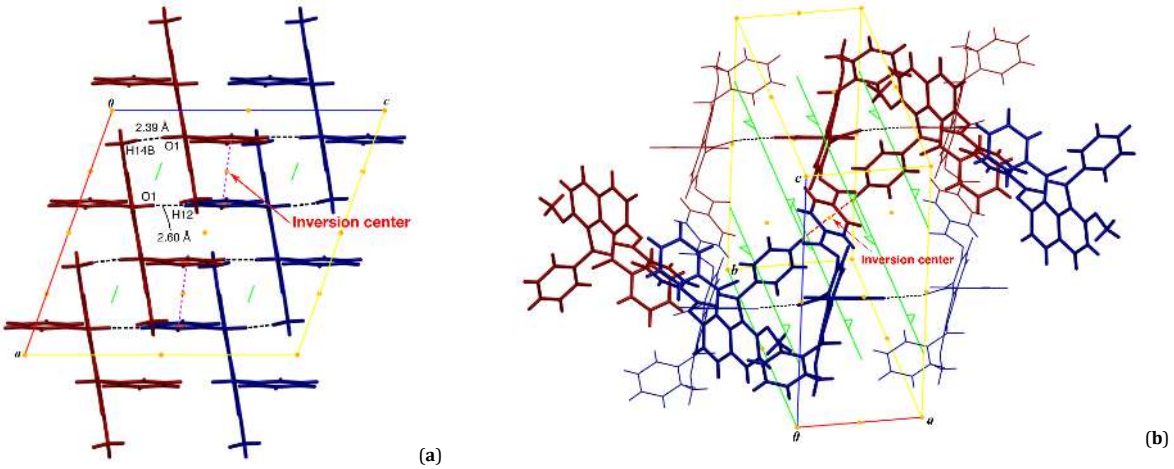

Figure 6. Molecular packing structures of (a) 1,8-dibenzoyl-2,7-dimethoxynaphthalene and (b) title compound with symmetry elements. *R,R*- and *S,S*-isomers are expressed as blue and red molecules, respectively.

The homologous compound has a sole value for the dihedral angle between each benzene ring and naphthalene and then lies on a two-fold rotation axis. The dihedral is closer to 90° than those of title compound. The high symmetricity of the spatial organization of the homologous compound indicates that two aroyl groups take suitably effective positions for forming π···π stacking interactions. On the other hand, in title compound, the π···π stacking interaction formation between aroyl groups is disturbed by steric hindrance brought about through the combination of bulkiness of largely congested two *peri*-benzoylnaphthalene units with terephthalate moiety. The benzoyl groups of *peri*-benzoylnaphthalene moiety in the title compound form effective C-H(sp²)···O=C and C-H(sp³)···O(-Me) non-classical hydrogen bonds instead of π···π stacking interactions (Figures 3b and 4). Furthermore, the terephthalate moiety on the inversion centre behaves as bidentate hydrogen acceptor of bidirectional C-H···π non-classical hydrogen bonds (Figure 4). This bidentate acceptant function of the terephthalate benzene ring is very unique behavior and substantially determines the whole crystal structure of the title compound. On the comparison with the homologous compound, the bidentate interaction is considered as transformation of the

π···π stacking interaction observed in the homologous compound through slipping of the two parallel benzene rings into the coplanar position accompanying with insertion of the benzene ring of terephthalate to result in achievement of synergetic enhancement of this type of noncovalent bonding interaction (Figures 6a and 6b). Consequently, different types of rather weak nonclassical hydrogen bonds cooperatively induce three-dimensional molecular network in the absence of determining support of effective non-covalent bonding interactions.

4. Conclusion

Conclusively, crystal structure of bis(1,8-dibenzoyl-7-methoxynaphthalen-2-yl) terephthalate and relationship among single molecular structure, accumulation structure, and effective influential non-covalent bonding interactions have been revealed. Two *peri*-benzoylnaphthalene units are situated centrosymmetrically due to the inversion centre on the terephthalate moiety. The molecular packing was stabilized by several weak non-covalent bonding interactions, *i.e.*, C-H(sp^2)···O=C, C-H(sp^3)C-H···OMe, and C-H(sp^2)···π non-classical hydrogen bonds. The terephthalate moiety forms bidirectional C-H(sp^2)···π non-classical hydrogen bonds as bidentate hydrogen acceptor. Comparison of spatial alignment in crystal with the homologous compound indicates that benzoyl groups in *peri*-benzoylnaphthalene unit could take a suitable conformation for forming several effective non-classical hydrogen bonds substitutable for impracticable π···π stacking interactions. The correlation among molecular structure, molecular packing structure, and weak interactions revealed in this study might be useful for the design of organic and polymer materials and understanding their properties.

Acknowledgements

The authors express their gratitude to Professor Keiichi Noguchi, Instrumentation Analysis Center, Tokyo University of Agriculture and Technology, for technical advice. This work was partially supported by Tokyo Ohka Foundation for The Promotion of Science and Technology and JSPS KAKENHI Grant No. JP20K05473.

Supporting information

CCDC-2063371 contains the supplementary crystallographic data for this paper. These data can be obtained free of charge via https://www.ccdc.cam.ac.uk/structures/, or by e-mailing data_request@ccdc.cam.ac.uk, or by contacting The Cambridge Crystallographic Data Centre, 12 Union Road, Cambridge CB2 1EZ, UK; fax: +44(0)1223-336033.

Disclosure statement

Conflict of interests: The authors declare that they have no conflict of interest.
Author contributions: All authors contributed equally to this work.
Ethical approval: All ethical guidelines have been adhered.

Funding

Tokyo Ohka Foundation for The Promotion of Science and Technology
https://dx.doi.org/10.13039/501100010795
Japan Society for the Promotion of Science
https://dx.doi.org/10.13039/501100001691

ORCID

Kikuko Iida
https://orcid.org/0000-0003-2580-0875
Rei Sakamoto
https://orcid.org/0000-0001-6558-3866
Kun Li
https://orcid.org/0000-0001-9112-7784
Miyuki Kobayashi
https://orcid.org/0000-0001-6292-9331
Hiroaki Iitsuka
https://orcid.org/0000-0003-3412-9139
Noriyuki Yonezawa
https://orcid.org/0000-0003-4696-5257
Akiko Okamoto
https://orcid.org/0000-0002-4148-0798

References

[1]. Desiraju, G. R. *Acc. Chem. Res.* **1991**, *24* (10), 290–296.
[2]. Desiraju, G. R. *Acc. Chem. Res.* **1996**, *29* (9), 441–449.
[3]. Steiner, T. *Chem. Commun. (Camb.)* **1997**, No. 8, 727–734.
[4]. Dang, L.-L.; Feng, H.-J.; Lin, Y.-J.; Jin, G.-X. *J. Am. Chem. Soc.* **2020**, *142* (44), 18946–18954.
[5]. Gao, Y.; Yin, Q.; Wang, Q.; Li, Z.; Cai, J.; Zhao, T.; Lei, H.; Wang, S.; Zhang, Y.; Shen, B. *Adv. Mater.* **2020**, *32* (48), e2005228.
[6]. Desiraju, G. R. *J. Mol. Struct.* **2003**, *656* (1–3), 5–15.
[7]. Desiraju, G. R. *Cryst. Growth Des.* **2011**, *11* (4), 896–898.
[8]. Aakeröy, C. B.; Seddon, K. R. *Chem. Soc. Rev.* **1993**, *22* (6), 397–407.
[9]. Desiraju, G. R. C. E. *The Design of Organic Solids*; Elsevier: Amsterdam, 1989.
[10]. Desiraju, G. R. *Angew. Chem. Int. Ed. Engl.* **1995**, *34* (21), 2311–2327.
[11]. Hisaki, I.; Nakagawa, S.; Ikenaka, N.; Imamura, Y.; Katouda, M.; Tashiro, M.; Tsuchida, H.; Ogoshi, T.; Sato, H.; Tohnai, N.; Miyata, M. *J. Am. Chem. Soc.* **2016**, *138* (20), 6617–6628.
[12]. Sasaki, T.; Ida, Y.; Hisaki, I.; Tsuzuki, S.; Tohnai, N.; Coquerel, G.; Sato, H.; Miyata, M. *Cryst. Growth Des.* **2016**, *16* (3), 1626–1635.
[13]. Budiman, Y. P.; Jayaraman, A.; Friedrich, A.; Kerner, F.; Radius, U.; Marder, T. B. *J. Am. Chem. Soc.* **2020**, *142* (13), 6036–6050.
[14]. Bondue, C. J.; Koper, M. T. M. *J. Am. Chem. Soc.* **2019**, *141* (30), 12071–12078.
[15]. Elsberg, J. G. D.; Anderson, S. N.; Tierney, D. L.; Reinheimer, E. W.; Berreau, L. M. *Dalton Trans.* **2021**, *50* (5), 1712–1720.
[16]. Wozniak, D. I.; Hicks, A. J.; Sabbers, W. A.; Dobereiner, G. E. *Dalton Trans.* **2019**, *48* (37), 14138–14155.
[17]. Kang, C.; Zhang, Z.; Wee, V.; Usadi, A. K.; Calabro, D. C.; Baugh, L. S.; Wang, S.; Wang, Y.; Zhao, D. *J. Am. Chem. Soc.* **2020**, *142* (30), 12995–13002.
[18]. Dionne, E. R.; Dip, C.; Toader, V.; Badia, A. *J. Am. Chem. Soc.* **2018**, *140* (32), 10063–10066.
[19]. Tian, X.; Xin, X.; Gao, Y.; Han, Z. *CrystEngComm* **2018**, *20* (11), 1588–1596.
[20]. Gargallo, R.; Aviñó, A.; Eritja, R.; Jarosova, P.; Mazzini, S.; Scaglioni, L.; Taborsky, P. *Spectrochim. Acta A Mol. Biomol. Spectrosc.* **2021**, *248* (119185), 119185.
[21]. Gomez-Jeria, J. S.; Robles-Navarro, A.; Kpotin, G. A.; Garro-Saez, N.; Gatica-Diaz, N. *Chem. Res. J.* **2020**, *5* (2), 32-52. https://chemrj.org/download/vol-5-iss-2-2020/chemrj-2020-05-02-32-52.pdf (accessed Apr 17, 2021).
[22]. Hahn, R.; Bohle, F.; Fang, W.; Walther, A.; Grimme, S.; Esser, B. *J. Am. Chem. Soc.* **2018**, *140* (51), 17932–17944.
[23]. Zuniga, M. A.; Alderete, J. B.; Jaña, G. A.; Jiménez, V. A. *J. Comput. Aided Mol. Des.* **2017**, *31* (7), 643–652.
[24]. Avdeeva, V. V.; Vologzhanina, A. V.; Ugolkova, E. A.; Minin, V. V.; Malinina, E. A.; Kuznetsov, N. T. *J. Solid State Chem.* **2021**, *296* (121989), 121989.
[25]. Kikkawa, S.; Okayasu, M.; Hikawa, H.; Azumaya, I. *Cryst. Growth Des.* **2021**, *21* (2), 1148–1158.
[26]. Kataeva, O.; Nohr, M.; Ivshin, K.; Hampel, S.; Büchner, B.; Knupfer, M. *Cryst. Growth Des.* **2021**, *21* (1), 471–481.
[27]. Awwadi, F. F.; Taher, D.; Kailani, M. H.; Alwahsh, M. I.; Odeh, F.; Rüffer, T.; Schaarschmidt, D.; Lang, H. *Cryst. Growth Des.* **2020**, *20* (2), 543–551.
[28]. Zeng, C.-H.; Wu, H.; Luo, Z.; Yao, J. *CrystEngComm* **2018**, *20* (8), 1123–1129.
[29]. Steiner, T.; Desiraju, G. R. *Chem. Commun. (Camb.)* **1998**, No. 8, 891–892.
[30]. Desiraju, G. R. *Chem. Commun. (Camb.)* **2005**, No. 24, 2995–3001.
[31]. Okamoto, A.; Yonezawa, N. *J. Synth. Org. Chem. Japan* **2015**, *73* (4), 339–360.

[32]. Okamoto, A.; Yonezawa, N. *Chem. Lett.* **2009**, *38* (9), 914–915.
[33]. Okamoto, A.; Mitsui, R.; Oike, H.; Yonezawa, N. *Chem. Lett.* **2011**, *40* (11), 1283–1284.
[34]. Okamoto, A.; Mitsui, R.; Watanabe, S.; Tsubouchi, T.; Yonezawa, N. *Int. J. Org. Chem. (Irvine)* **2012**, *02* (03), 194–201.
[35]. Ogata, K.; Mido, T.; Siqingaowa; Noguchi, K.; Yonezawa, N.; Okamoto, A. *Chem. Lett.* **2019**, *48* (12), 1522–1525.
[36]. Mido, T.; Iitsuka, H.; Kobayashi, M.; Noguchi, K.; Yonezawa, N.; Okamoto, A. *Chem. Lett.* **2020**, *49* (3), 295–298.
[37]. Nakaema, K.; Watanabe, S.; Okamoto, A.; Noguchi, K.; Yonezawa, N. *Acta Crystallogr. Sect. E Struct. Rep. Online* **2008**, *64* (Pt 5), o807.
[38]. Armarego, W. L. F.; Perrin, D. D. *Purification of Laboratory Chemicals*, Fourth Edition; Reed Educational and Professional Publishing Ltd: Oxford, 1996.
[39]. Domasevitch, K. V.; Solntsev, P. V.; Krautscheid, H.; Zhylenko, I. S.; Rusanov, E. B.; Chernega, A. N. *Chem. Commun. (Camb.)* **2012**, *48* (47), 5847–5849.
[40]. Kato, Y.; Nagasawa, A.; Hijikata, D.; Okamoto, A.; Yonezawa, N. *Acta Crystallogr. Sect. E Struct. Rep. Online* **2010**, *66* (10), o2659–o2659.
[41]. Nagasawa, A.; Mitsui, R.; Kato, Y.; Okamoto, A.; Yonezawa, N. *Acta Crystallogr. Sect. E Struct. Rep. Online* **2010**, *66* (10), o2677–o2677.
[42]. Rigaku. *PROCESS-AUTO*. Rigaku Corporation, Tokyo, Japan, 1998.
[43]. Rigaku. *CrystalStructure*. Rigaku Corporation, Tokyo, Japan, 2010.
[44]. Burla, M. C.; Caliandro, R.; Camalli, M.; Carrozzini, B.; Cascarano, G. L.; De Caro, L.; Giacovazzo, C.; Polidori, G.; Siliqi, D.; Spagna, R. *J. Appl. Crystallogr.* **2007**, *40* (3), 609–613.
[45]. Sheldrick, G. M. *Acta Crystallogr. C Struct. Chem.* **2015**, *71* (1), 3–8.